Structural Rheology of Microphase Separated Diblock Copolymers

Ryota TAMATE, Kohtaro YAMADA[1], Jorge VIÑALS[2], and Takao OHTA[*]

Department of Physics, Kyoto University, Kyoto 606-8502
[1]*Department of Chemistry, Tokyo Metropolitan University, Tokyo 192-0397*
[2]*McGill Institute for Advanced Materials and Department of Physics, McGill University,*
Montreal, QC H3A 2T8, Canada

We formulate a viscoelastic theory for interconnected microphase separated structures such as a double gyroid in diblock copolymer melts. We consider the energy increase and the energy dissipation due to the deformation of interconnected periodic domains. The dominant elastic part agrees with previous analytical results obtained by a phase formulation of deformations. It is shown that a viscous response also appears which is mainly due to two relaxation modes of the gyroid.

1. Introduction

One of the characteristic features of soft matter is that various mesoscopic phases of different symmetry appear in thermal equilibrium. For example, the elastic and viscoelastic properties of the smectic phase of liquid crystals have been investigated both theoretically and experimentally for many years.[1] The latter is essentially one dimensional order and therefore, the theoretical formulation of dynamics is not very complicated.

As is well known, however, there are interconnected bicontinuous periodic structures such as (double) gyroid structure, (double) diamond structure and primitive surface structure in block copolymers and water/surfactant mixtures.[2–6] Rheological measurements have also been performed for these structures, and such experiments provide us with evidence of the morphological transitions.[7,8]

The linear elasticity of a gyroid structure has been studied theoretically. Tyler and Morse have evaluated numerically the elastic moduli of a gyroid by means of self-consistent mean field theory.[9] Two of the present authors (KY and TO) have calculated analytically the same elastic constants in the weak segregation limit,[10] and found simple relations among the three elastic moduli which are not inconsistent with the numerical results of Tyler and Morse.[9]

There is a fairly large number of computer simulations of the rheological behavior of microphase separated structures.[11,12] However, most of the studies are limited to the lamellar or hexagonal structures. To the authors' knowledge, there are no theoretical studies of the viscous response of interconnected structures such as gyroid and diamond phases.

The purpose of the present paper is to formulate a linear visco-elastic theory of interconnected periodic network structures under oscillatory shear flow. We focus our attention on structural rheology, that is, on free energy increase and dissipation due to domain deformation. We explore the universal rheological properties of interconnected periodic networks, independently of the molecular details of the constituents. We use a coordinate transformation introduced by Drolet, Chen, and Viñals,[13] which makes it possible to evaluate stress–strain relations by solving a set of the amplitude equations for the mesoscopic structures. We employ a mode expansion method and numerically solve the 18 amplitude equations describing a gyroid.[14] One of the advantages of the present theory is that large computer simulations are unnecessary even though the interconnected network structure is fairly complicated to represent mathematically. We show analytically that the elastic limit agrees with previous results.[10]

As mentioned above, since our aim is to formulate the linear visco-elasticity as analytically as possible, we introduce several idealized conditions. First of all, we do not consider large deformations that might cause domain reconnection. We further assume that the interconnected structure contains neither grain boundaries nor dislocations. Finally, hydrodynamic interactions are not considered. They are important in water/surfactant mixtures, but not as relevant in block copolymer melts. As mentioned above, we only consider the deformation of domains under shear strain, hence the elasticity or viscosity due to individual polymer chains are not considered. This simplification is justified if the characteristic time of domain deformation is much larger than the characteristic relaxation times of a polymer chain. We shall return to these issues in the final section.

In the next section (§2) we start with the time-evolution equation for microphase separation in diblock copolymers under shear flow, including the expression of the stress tensor. Numerical results for stress–strain relations are obtained in §3, whereas analytical results for the visco-elasticity of a gyroid structure are given in §4. A discussion is presented in §5, where some of the approximations and assumptions employed are examined.

2. Free Energy Functional and Kinetic Equation under Shear Flow

The simplest nontrivial free energy for microphase separation in A–B type diblock copolymers is given by[15]

$$F\{\psi\} = \int d\mathbf{r} \left\{ \frac{K}{2} [\nabla \psi(\mathbf{r})]^2 - \frac{\theta}{2} \psi(\mathbf{r})^2 + \frac{g}{4} \psi(\mathbf{r})^4 \right\}$$
$$+ \frac{\alpha}{2} \int d\mathbf{r} \int d\mathbf{r}' \, G(\mathbf{r} - \mathbf{r}')[\psi(\mathbf{r}) - \bar{\psi}][\psi(\mathbf{r}') - \bar{\psi}]. \quad (1)$$

Throughout the present paper, we use $k_BT = 1$. The variable ψ is the local concentration difference of A and B monomers.

*E-mail: takao@scphys.kyoto-u.ac.jp

The constants K, θ, g, and α are all positive in the microphase separated state. The spatial average of ψ enters in the last term as $\bar{\psi}$. The Green function G is defined through

$$-\nabla^2 G(\boldsymbol{r} - \boldsymbol{r}') = \delta(\boldsymbol{r} - \boldsymbol{r}'). \qquad (2)$$

The linear elasticity of a gyroid has been formulated starting from the free energy (1). The elastic energy is given by[10]

$$F\{u\} = \frac{1}{2}\int \mathrm{d}\boldsymbol{r}\big[K_{11}\big(u_{xx}{}^2 + u_{yy}{}^2 + u_{zz}{}^2\big) \\ + 2K_{12}\big(u_{xx}u_{yy} + u_{yy}u_{zz} + u_{zz}u_{xx}\big) \\ + 4K_{44}\big(u_{xy}{}^2 + u_{yz}{}^2 + u_{zx}{}^2\big)\big], \qquad (3)$$

where the strain tensor $u_{\alpha\beta}$ is defined by

$$u_{\alpha\beta} \equiv \frac{1}{2}(\nabla_\beta u_\alpha + \nabla_\alpha u_\beta). \qquad (4)$$

The elastic moduli are evaluated in the weak segregation regime as

$$K_{11} = 16q_0{}^2\left(\phi_a{}^2 + \frac{2}{3}\phi_b{}^2\right), \qquad (5)$$

and

$$K_{12} = K_{44} = 8q_0{}^2\left(\phi_a{}^2 + \frac{2}{3}\phi_b{}^2\right) = \frac{1}{2}K_{11}, \qquad (6)$$

where q_0 is the magnitude of the basic reciprocal vector, and ϕ_a and ϕ_b are the amplitude of ψ for a gyroid. These are determined by eqs. (31) and (22) with $\sigma_{xz} = \gamma(t) = 0$ below. Note that there is a particular relation among the elastic constants, which is a general property of a mesophase with cubic symmetry in the weak segregation limit.[10]

In the present dynamical theory, the fundamental quantity is the stress tensor. It can be derived from the free energy (1) as[16]

$$\sigma_{\alpha\beta} = -\frac{K}{V}\int \mathrm{d}\boldsymbol{r}\, \frac{\partial\psi}{\partial r_\alpha}\frac{\partial\psi}{\partial r_\beta} \\ + \frac{\alpha}{2V}\int \mathrm{d}\boldsymbol{r}\int \mathrm{d}\boldsymbol{r}'\, r_\beta \frac{\partial G(\boldsymbol{r})}{\partial r_\alpha}\psi\left(\boldsymbol{r}' + \frac{\boldsymbol{r}}{2}\right)\psi\left(\boldsymbol{r}' - \frac{\boldsymbol{r}}{2}\right), \qquad (7)$$

where $\alpha \neq \beta$ and V is the system volume. This formula is employed as follows. The time-evolution of ψ is evaluated under a time-dependent strain. Substituting it into eq. (7) gives us the stress–strain relation as formulated below.

In the weak segregation regime, the kinetic equation governing the local concentration ψ is given by

$$\frac{\partial\psi}{\partial t} + \boldsymbol{v}\cdot\nabla\psi = L\nabla^2\frac{\delta F}{\delta\psi} \\ = L[\nabla^2(-K\nabla^2\psi - \theta\psi + g\psi^3) \\ - \alpha(\psi - \bar{\psi})], \qquad (8)$$

where the constant L is an Onsager coefficient. We have added an advection term which incorporates the imposed external shear flow $\boldsymbol{v}$. By introducing dimensionless quantities, $t' = L\alpha t$, $x_i' = (\alpha/K)^{1/4}x_i$, and $\psi' = g^{1/2}/(\alpha K)^{1/4}\psi$, eq. (8) becomes

$$\frac{\partial\psi'}{\partial t'} + \boldsymbol{v}'\cdot\nabla'\psi' \\ = \nabla'^2\left(-\nabla'^2\psi' - \frac{\theta}{(\alpha K)^{1/2}}\psi' + \psi'^3\right) - (\psi' - \bar{\psi}'). \qquad (9)$$

Hereafter we shall omit the primes and replace $\theta/(\alpha K)^{1/2}$ by θ.

Now we suppose that an oscillatory shear flow is applied given by

$$\boldsymbol{v} = (\dot{\gamma}(t)z, 0, 0), \qquad (10)$$

with

$$\gamma(t) = \gamma_0\sin\omega t, \qquad (11)$$

where $\dot{\gamma}(t) = \mathrm{d}\gamma/\mathrm{d}t$, γ_0 stands for the strain amplitude and ω is the strain frequency. If one introduces the new coordinate which moves with the flow

$$x_1 = x - \gamma(t)z, \qquad (12)$$
$$x_2 = y, \qquad (13)$$
$$x_3 = z, \qquad (14)$$

the evolution equation (9) can be written as[13]

$$\frac{\partial\psi}{\partial t} = \hat{\nabla}^2(-\theta\psi + \psi^3 - \hat{\nabla}^2\psi) - (\psi - \bar{\psi}), \qquad (15)$$

where

$$\hat{\nabla}^2 = [1 + \gamma^2(t)]\frac{\partial^2}{\partial x_1^2} - 2\gamma(t)\frac{\partial^2}{\partial x_1\partial x_3} + \frac{\partial^2}{\partial x_3^2} + \frac{\partial^2}{\partial x_2^2}. \qquad (16)$$

In terms of dimensionless quantities, the stress tensor (7) can be represented after Fourier transform as

$$\sigma_{\alpha\beta} = -\sum_{\boldsymbol{q}\neq\boldsymbol{0}} q_\alpha q_\beta\left(1 - \frac{1}{q^4}\right)|\psi_{\boldsymbol{q}}(t)|^2. \qquad (17)$$

Therefore if one solves the time-evolution equation (9) with shear flow, the stress–strain response can be obtained from formula (17). This was carried out by numerical simulations for macrophase separation[17] and microphase separation[11] in two dimensions. In the present paper, we solve eq. (15) to investigate the viscoelastic properties of microphase separated structures.

It should be noted that, although the shear flow in eq. (10) is in the $(1, 0, 0)$ direction, the above theory can be applied to arbitrary direction of shear flow. In fact, we have carried out numerical simulations for the $(1, 0, 0)$ flow and the $(1, 1, 1)$ flow. However, in the next section, we shall show the results of the $(1, 0, 0)$ flow since there are no essential difference between the two cases.

3. Numerical Simulations of Viscoelastic Response

A double gyroid structure is one of the bicontinuous network structures observed in soft matter. It appears as an equilibrium state in microphase separation of diblock copolymers. In the weak segregation regime, we may represent the double gyroid structure as[14]

$$\psi(\boldsymbol{r}) = \bar{\psi} + \left(\sum_{j=1}^{12} A_j\mathrm{e}^{i\boldsymbol{q}_j\cdot\boldsymbol{r}} + \sum_{k=1}^{6} B_k\mathrm{e}^{i\boldsymbol{p}_k\cdot\boldsymbol{r}} + \mathrm{c.c.}\right), \qquad (18)$$

where $\boldsymbol{r} = (x_1, x_2, x_3)$ is a point moving with the flow as introduced in the previous section. The 18 reciprocal lattice vectors are given by

$$\boldsymbol{q}_1 = C_Q(2, -1, 1), \qquad \boldsymbol{q}_2 = C_Q(-2, 1, 1),$$
$$\boldsymbol{q}_3 = C_Q(-2, -1, 1), \qquad \boldsymbol{q}_4 = C_Q(2, 1, 1),$$
$$\boldsymbol{q}_5 = C_Q(-1, -2, 1), \qquad \boldsymbol{q}_6 = C_Q(1, -2, 1),$$
$$\boldsymbol{q}_7 = C_Q(-1, 2, 1), \qquad \boldsymbol{q}_8 = C_Q(1, 2, 1),$$

$$\boldsymbol{q}_9 = C_Q(1,-1,-2), \quad \boldsymbol{q}_{10} = C_Q(1,1,-2),$$
$$\boldsymbol{q}_{11} = C_Q(-1,1,-2), \quad \boldsymbol{q}_{12} = C_Q(-1,-1,-2),$$
$$\boldsymbol{p}_1 = C_P(2,2,0), \quad \boldsymbol{p}_2 = C_P(2,-2,0),$$
$$\boldsymbol{p}_3 = C_P(0,2,2), \quad \boldsymbol{p}_4 = C_P(0,-2,2),$$
$$\boldsymbol{p}_5 = C_P(2,0,2), \quad \boldsymbol{p}_6 = C_P(-2,0,2), \tag{19}$$

with $C_Q = Q/\sqrt{6}$ and $C_P = P/2\sqrt{2}$ where Q and P denote the absolute value of $\boldsymbol{q}_j$ and $\boldsymbol{p}_k$ respectively and satisfy $Q^2 = (3/4)P^2$.

The time evolution equations for the amplitudes A_j ($j = 1, \ldots, 12$) and B_k ($k = 1, \ldots, 6$) are obtained by substituting (18) into eq. (15) and neglecting higher harmonics.[14] This is justified in the weak segregation limit. For example, the amplitude equation for A_1 is given under oscillatory shear flow by

$$\frac{dA_1}{dt} = [\theta q_1(t)^2 - q_1(t)^4 - 1]A_1$$
$$- q_1(t)^2 \Bigg[3(\bar{\psi}^2 - A_1^2)A_1 + 6\left(\sum_{j=1}^{12} A_j^2 + \sum_{k=1}^{6} B_k^2\right)A_1$$
$$+ 6\bar{\psi}A_3B_4 + 6\bar{\psi}A_7A_{12} + 6A_1B_2B_5 + 6A_2A_3A_4$$
$$+ 6A_2A_5A_8 + 6A_2A_6A_7 + 6A_3B_1B_2 + 6A_3B_1B_5$$
$$+ 6A_3B_2B_6 + 6A_3B_5B_6 + 6A_4A_9A_{10} + 6A_4A_{11}A_{12}$$
$$+ 6A_5A_{10}B_2 + 6A_5A_{10}B_5 + 6A_5A_{12}B_6 + 6A_6A_9B_3$$
$$+ 6A_6A_9B_6 + 6A_6A_{11}B_2 + 6A_6A_{11}B_4 + 6A_6A_{11}B_5$$
$$+ 6A_7A_{10}B_1 + 6A_8A_9B_4 + 6A_8A_{11}B_1 + 6A_8A_{11}B_3 \Bigg], \tag{20}$$

where $q_1^2(t)$ is defined by

$$q_1^2(t) = q_{1x}^2 + q_{1y}^2 + [q_{1z} - \gamma(t)q_{1x}]^2. \tag{21}$$

Equation (20) has to be supplemented by the other 17 equations for the remaining amplitudes.

We find stress–strain relations for the oscillatory shear (10) by numerically solving the coupled set of amplitude equations, and by using the expression of the stress tensor derived from eq. (17)

$$\sigma_{xz} = -2\sum_{j=1}^{12} q_{jx}[q_{jz} - \gamma(t)q_{jx}]\left[1 - \frac{1}{q_j^4(t)}\right]A_j^2$$
$$- 2\sum_{k=1}^{6} p_{kx}[p_{kz} - \gamma(t)p_{kx}]\left[1 - \frac{1}{p_k^4(t)}\right]B_k^2. \tag{22}$$

The result is shown in Fig. 1(a) for $\omega = 0.1$. The storage modulus $G'(\omega)$ and the loss modulus $G''(\omega)$ are now defined by the following equation

$$\sigma_{xz} = \gamma_0[G'(\omega)\sin\omega t + G''(\omega)\cos\omega t]$$
$$+ (\text{higher harmonics}). \tag{23}$$

Note that a nonlinear dependence on γ_0 in G' and G'' is allowed in this definition. Because the elastic component of the response is dominant [see Fig. 1(a)], and almost independent of ω in the limit $\omega \to 0$, we also introduce a storage modulus difference $\Delta G'(\omega) = G'(\omega) - G'(0.00001)$. Figure 1(b) shows $G'(\omega)$, $G''(\omega)$, and $\Delta G'(\omega)$. It is evident that the elastic modulus G' is much larger than the loss modulus G''. We note that the moduli $\Delta G'$ and G'' exhibit a frequency dependence characteristic of Maxwell vis-
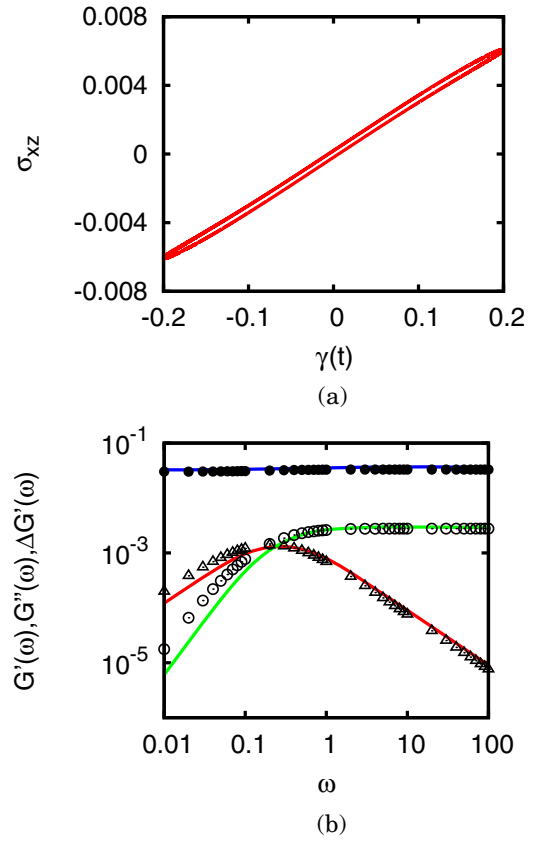

(a)

(b)

Fig. 1. (Color online) (a) Stress–strain curves for $\theta = 2.2$, $\bar{\psi} = 0.1$, $\gamma_0 = 0.2$, and frequency $\omega = 0.1$. (b) $G'(\omega)$ (dark circles), $\Delta G'(\omega)$ (open circles), and $G''(\omega)$ (triangles) for $\gamma_0 = 0.2$. The solid curves are obtained from eqs. (47) and (48).
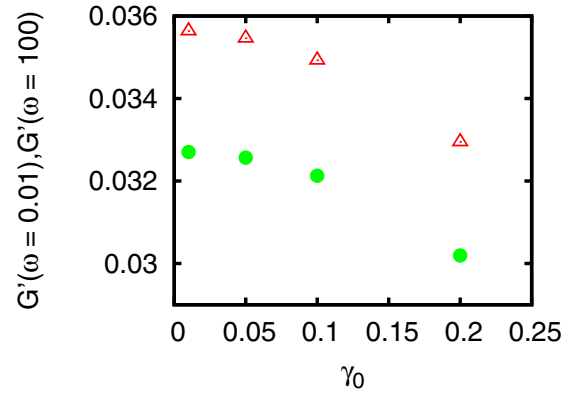

Fig. 2. (Color online) Nonlinear relation between $G'(\omega)$ and γ_0 for $\omega = 100$ (triangles) and $\omega = 0.01$ (circles).

coelasticity. This is illustrated by the solid curves in Fig. 1(b), which we will derive analytically in the next section.

In Fig. 2 we have plotted the γ_0 dependence of G' obtained numerically for $\omega = 100$ and $\omega = 0.01$. It is interesting to note that the modulus G' decreases as the strain amplitude γ_0 is increased. We have evaluated the elastic free energy to fourth order in the strain and found that the elastic coefficient for the shear deformation is negative in the weak segregation limit as is consistent with the above observation.

4. Theory of Viscoelastic Response

In this section, we interpret the results shown in Fig. 1 theoretically. First we write eq. (18) as

$$\psi(\boldsymbol{r}, t) = \bar{\psi} + 2 \sum_{j=1}^{18} A_j(t) \cos(\boldsymbol{q}_j \cdot \boldsymbol{r}), \tag{24}$$

where we have used the notation $A_j = B_{j-12}$ and $\boldsymbol{q}_j = \boldsymbol{p}_{j-12}$ for $j = 13, \ldots, 18$. The evolution equations for the amplitudes are given from eq. (15) by

$$\frac{dA_j}{dt} = Q[q_j(t)^2]A_j - q_j(t)^2 W_j(\boldsymbol{A}), \tag{25}$$

where

$$Q(q^2) = (\theta - 3\bar{\psi}^2)q^2 - q^4 - 1, \tag{26}$$

and

$$q(t)^2 = q_x^2 + q_y^2 + [q_z - (\gamma_0 \sin \omega t)q_x]^2. \tag{27}$$

The terms $W_j(\boldsymbol{A})$ with $\boldsymbol{A} \equiv (A_1, A_2, \ldots)$ arise from nonlinear couplings among the amplitudes.

We next expand the amplitudes, $W_j(\boldsymbol{A})$ and $Q(q^2)$ as

$$A_j = A_j^{(0)} + \gamma_0 A_j^{(1)} + \gamma_0^2 A_j^{(2)} + O(\gamma_0^3), \tag{28}$$

$$W_j = W_j^{(0)}(\boldsymbol{A}^{(0)}) + \gamma_0 \sum_{k=1}^{18} W_{jk}^{(1)}(\boldsymbol{A}^{(0)})A_k^{(1)} + O(\gamma_0^2), \tag{29}$$

$$Q(q^2) = Q^{(0)}(q^2) + \gamma_0 Q^{(1)} + O(\gamma_0^2). \tag{30}$$

Substituting this into the amplitude equations, we obtain the zeroth order solution as

$$0 = Q^{(0)}(q_j^2)A_j^{(0)} - q_j^2 W_j^{(0)}(\boldsymbol{A}^{(0)}). \tag{31}$$

The solutions are obtained numerically and have been found to separated into two groups as

$$|A_j^{(0)}| \equiv \phi_a \quad (j = 1, \ldots, 12), \tag{32}$$

$$A_j^{(0)} \equiv \phi_b \quad (j = 13, \ldots, 18), \tag{33}$$

where $\phi_a = 0.06456$ for $j = 1, 4, 5, 8, 9, 12$ and $\phi_a = -0.06456$ for $j = 2, 3, 6, 7, 10, 11$ and $\phi_b = 0.02353$. Another set of $\pm\phi_a$ is also possible depending on the initial conditions such as $\phi_a = 0.06456$ for $j = 1, 2, 5, 6, 11, 12$ and $\phi_a = -0.06456$ for $j = 3, 4, 7, 8, 9, 10$. These are evaluated for the parameters $\theta = 2.2$, $\bar{\psi} = 0.1$.

At first order, the governing equation for the first amplitude is

$$\frac{dA_j^{(1)}}{dt} = Q^{(0)}(q_j^2)A_j^{(1)} - q_j^2 \sum_{k=1}^{18} W_{jk}^{(1)}(\boldsymbol{A}^{(0)})A_k^{(1)}$$
$$- 2q_{jx}q_{jz}\sin \omega t$$
$$\times [(\theta - 3\bar{\psi}^2 - 2q_j^2)A_j^{(0)} - W_j^{(0)}(\boldsymbol{A}^{(0)})]. \tag{34}$$

By the notation introducing

$$D_{jk}^{(1)} = \delta_{jk}Q^{(0)}(q_j^2) - q_j^2 W_{jk}^{(1)}(\boldsymbol{A}^{(0)}), \tag{35}$$

and

$$h_j^{(1)} = -2q_{jx}q_{jz}[(\theta - 3\bar{\psi}^2 - 2q_j^2)A_j^{(0)} - W_j^{(0)}(\boldsymbol{A}^{(0)})]$$
$$= 2q_{jx}q_{jz}q_j^2\left(1 - \frac{1}{q_j^4}\right)A_j^{(0)}, \tag{36}$$

eq. (34) can be written as

$$\frac{dA_j^{(1)}}{dt} = \sum_{k=1}^{18} D_{jk}^{(1)}A_k^{(1)} + h_j^{(1)}\sin \omega t. \tag{37}$$

Equation (37) can be solved by diagonalizing the coefficient matrix $D_{jk}^{(1)}$ as $P^{-1}D^{(1)}P$ with a regular matrix P. Introducing $\hat{\boldsymbol{A}}^{(1)} = P^{-1}\boldsymbol{A}^{(1)}$ and $\hat{\boldsymbol{h}}^{(1)} = P^{-1}\boldsymbol{h}^{(1)}$ we have from eq. (37)

$$\frac{d}{dt}\hat{A}_i^{(1)} = -\lambda_i \hat{A}_i^{(1)} + \hat{h}_i^{(1)}\sin \omega t, \tag{38}$$

where $-\lambda_i$ are the eigenvalues of $D^{(1)}$. We have found by numerical diagonalization that there are eight modes with different eigenvalues. Solving eq. (38), we obtain

$$A_i^{(1)}(t) = \sum_{j=1}^{18} \alpha_{ij}\left[\frac{(\omega/\lambda_j)^2}{1 + (\omega/\lambda_j)^2}\sin \omega t \right.$$
$$\left. + \frac{\omega/\lambda_j}{1 + (\omega/\lambda_j)^2}\cos \omega t - \sin \omega t\right]$$
$$+ \sum_{j=1}^{18} P_{ij}C_j e^{-\lambda_j t}, \tag{39}$$

where

$$\alpha_{ij} = -P_{ij}\frac{\hat{h}_j^{(1)}}{\lambda_j} = -\frac{P_{ij}}{\lambda_j}\sum_{k=1}^{18}(P^{-1})_{jk}h_k^{(1)}. \tag{40}$$

As mentioned at the end of §2, the present theory can be applied to the shear flow with any directions and hence all of the complex moduli are evaluated. However, since no essential difference appears in the various moduli, we here present only the expression of σ_{xz}. Substituting (39) into the stress tensor (17), we obtain

$$\sigma_{xz} = -2\sum_{i=1}^{18} q_{ix}[q_{iz} - \gamma(t)q_{ix}]\left[1 - \frac{1}{q_i^4(t)}\right]$$
$$\times [A_i^{(0)} + \gamma_0 A_i^{(1)} + O(\gamma_0^2)]^2. \tag{41}$$

Looking only at terms linear in the strain amplitude γ_0, we find

$$\sigma_{xz} = \sigma_{\text{phase}} + \sigma_{xz}', \tag{42}$$

where σ_{phase} is the stress arising from a change in wave number [from the first line of eq. (41) at constant amplitude]

$$\sigma_{\text{phase}} = 8\gamma_0 q_0^2\left(\phi_a^2 + \frac{2}{3}\phi_b^2\right)\sin \omega t. \tag{43}$$

This stress is in phase with the strain $\gamma(t)$, and the proportional constant agrees with K_{44} of eq. (6).[10] The other term σ_{xz}' rises from amplitude corrections, and is given by

$$\sigma_{xz}' = -4\gamma_0 \sum_{i=1}^{18} q_{ix}q_{iz}\left(1 - \frac{1}{q_i^4}\right)A_i^{(0)}A_i^{(1)}, \tag{44}$$

which is given asymptotically from eq. (39) by

$$\sigma_{xz}' = \gamma_0 \sum_{j=1}^{18} \Gamma_j\left[\frac{(\omega/\lambda_j)^2}{1 + (\omega/\lambda_j)^2}\sin \omega t \right.$$
$$\left. + \frac{\omega/\lambda_j}{1 + (\omega/\lambda_j)^2}\cos \omega t - \sin \omega t\right], \tag{45}$$

where

$$\Gamma_j = -4\sum_{i=1}^{18} q_{ix}q_{iz}\left(1 - \frac{1}{q_i^4}\right)A_i^{(0)}\alpha_{ij}. \tag{46}$$

In summary, we obtain the following expressions for the storage modulus G' and the loss modulus G''

$$G' = \sum_{j=1}^{8} \Gamma_j \left[\frac{(\omega/\lambda_j)^2}{1 + (\omega/\lambda_j)^2} - 1 \right] + 8q_0^2 \left(\phi_a^2 + \frac{2}{3} \phi_b^2 \right), \quad (47)$$

$$G'' = \sum_{j=1}^{8} \Gamma_j \left[\frac{\omega/\lambda_j}{1 + (\omega/\lambda_j)^2} \right], \quad (48)$$

where we have taken into account that there are only eight independent modes. The coefficients Γ_j have been properly renumbered. Note that the moduli (47) and (48) do not contain the strain magnitude γ_0, and therefore they constitute the linear response to the oscillatory shear.

The eigenvalues and the eigenvectors have been evaluated numerically for $\theta = 2.2$ and $\bar{\psi} = 0.1$. There are two dominant modes

$$\lambda_1 = 0.1627, \quad \Gamma_1 = 1.454 \times 10^{-3}, \quad (49)$$

$$\lambda_2 = 0.4465, \quad \Gamma_2 = 1.501 \times 10^{-3}. \quad (50)$$

Both modes are triply degenerate. The values of Γ_k for other modes are small and we neglect them. There is one extra mode that has a small eigenvalue, $\lambda_0 = 0.07375$. However the corresponding coefficient is quite small as $\Gamma_0 = -9.12145 \times 10^{-6}$. Therefore this contribution to the stress tensor is at most 3% of the contribution from those modes given by (49) and (50), and we have also neglected it.

We have tried to represent the deformations associated with the two modes (49) and (50). However, we have no simple and appropriate way of displaying the three-dimensional deformed structure. For the reader's convenience, the deformed patterns for several conditions are available on the web site.[18]

Our results for the moduli (47) and (48) with (49) and (50) are plotted in Fig. 1(b) together with the numerical results described earlier. The small discrepancy at low frequencies between the results of eqs. (47) and (48) and those from eq. (22) can be attributed to the fact that the solid curve is purely linear response whereas $\Delta G'(\omega)$ (open circles) and $G''(\omega)$ (triangles) contain nonlinear effects. We have verified that the agreement between the two calculations is better for smaller γ_0, e.g., for $\gamma_0 = 0.1$ (results not shown).

5. Discussion

We have formulated the rheology of a gyroid structure, and evaluated the storage and loss moduli both numerically and analytically from an amplitude equation expansion. The elastic part arising from wavelength compression agrees with previous results.[10] Periodic amplitude modulation under an oscillatory strain give rise to additional contributions to the moduli. The analytical calculation shows that both storage and loss moduli can be represented in terms of a Maxwell model with two relaxation rates in the present case. Although the loss modulus is small compared with its elastic counterpart [$G''/G' \sim 10^{-2}$ for $\omega = 0.2$ as in Fig. 1(b)], our results are new for the gyroid phase with its regular but complicated network structure. We note that the small values of G'' can be detected experimentally and that, in fact, the ratio $G''/G' \sim 10^{-2}$ for a gyroid has been reported for a shear strain of 1% and a shear frequency of 1 rad/s.[7]

As emphasized in the Introduction, we are concerned here with the universal rheological properties of bi (or tri)-continuous structures which are basic mesophases in soft matter, not only in block copolymers but also in water-surfactant mixtures. The present formulation can be straightforwardly extended to other interconnected structures such as double diamond and primitive surface structures, and therefore used to investigate the general rheological response to domain deformation in complex phases. In reality, however, there are number of effects specific to each system that would have to be considered: finite relaxation times of individual polymer chains, a concentration dependence of the Onsager coefficient, and possible hydrodynamics effects. In the following, we qualitatively examine each of these effects.

First of all, we note that a concentration dependence of the Onsager coefficient is not important for the linear response to domain deformations as we have studied here. Second, we address possible effects arising from the relaxation of individual polymer chains. It should be kept in mind that we are considering the weak segregation regime near the microphase separation temperature, and therefore the monomer concentration variation is almost sinusoidal with no sharp interfaces. Since the radius of gyration of a chain R_g is the only characteristic length scale in the weak segregation limit, the domain period ℓ should be of the order of R_g. When the chains are short, Rouse dynamics in melts provides us with a relaxation time $t_R \propto N^2$ with N the molecular weight.[19] The last term of eq. (8) shows that $t_{TDGL} = (L\alpha)^{-1}$ has dimensions of time. Since L is independent of the molecular weight for the Rouse dynamics[20] and $\alpha \propto N^{-2}$,[15] t_{TDGL} has the same N-dependence as t_R. However, we note that the characteristic relaxation time of deformed domains becomes large near the stability limit of the gyroid so that the relaxation of the individual chains is not relevant as long as the molecular weight is not extremely large (so that Rouse scaling with N holds).

Monomer concentration fluctuations are generally not relevant in polymer melts, except for very vicinity of the order–disorder transition point $\bar{\psi} = 0$ and $\theta = 2.0$. The gyroid structure appears in the weak segregation regime, but for $\theta \geq 2.17$ and $|\bar{\psi}| \geq 0.095$.[21] Therefore, we expect that fluctuation effects can be neglected in the dynamics of a gyroid.

We finally estimate the magnitude of hydrodynamic interactions on the evolution of monomer concentration ψ. In general, we have,

$$\frac{\partial \psi}{\partial t} + \nabla \cdot (\boldsymbol{v}\psi) = L\nabla^2 \frac{\delta F}{\delta \psi}. \quad (51)$$

In the limit of zero Reynolds number (overdamped motion), and assuming that the flow in the melt is Newtonian (see ref. 22 for a discussion of non Newtonian corrections in lamellar phases), the local velocity field $\boldsymbol{v}$ is given by

$$\boldsymbol{v}(\boldsymbol{r},t) = \frac{1}{\eta} \int d\boldsymbol{r}' \, \boldsymbol{T}(\boldsymbol{r},\boldsymbol{r}') \cdot \left[(\nabla'\psi) \frac{\delta F}{\delta \psi(\boldsymbol{r}')} \right], \quad (52)$$

where $\boldsymbol{T}$ is the Oseen tensor, and η the shear viscosity. The ratio of advection to monomer concentration diffusion in eq. (51) is determined by the dimensionless group

$$H_Y = \frac{\ell^2 (\delta\psi)^2}{\eta L(\bar{\psi})}, \quad (53)$$

J. Phys. Soc. Jpn., Vol. 77, No. 3

R. Tamate *et al.*

where $\delta\psi$ is the amplitude of concentration variations in the microphase separated phase. If H_Y is sufficiently small, hydrodynamic effects can be neglected. In order to estimate the value of this dimensionless group, we note the fact that the melt viscosity is proportional to $R_g^2 \propto N$,[19] and obtain[17]

$$\eta L \simeq R_g^2 \simeq N, \tag{54}$$

and hence

$$H_Y \simeq \frac{\ell^2 (\delta\psi)^2}{R_g^2} \propto (\delta\psi)^2. \tag{55}$$

Therefore, hydrodynamic effects are not important in the weak segregation regime in which the scale of spatial variations $\delta\psi$ is small. On the other hand, the characteristic length ℓ should be of the order of the period of the structure in the strong segregation regime. The period is related to the molecular weight as $\ell \simeq N^{2/3}$, and H_Y would become large for large N. Therefore hydrodynamic interactions cannot be ignored in the strong segregation regime.

In the case of reptation dynamics we have

$$\eta L \simeq R_g^2 N / N_e, \tag{56}$$

since $L \simeq R_g^2 N_e / N^2$,[20] and $\eta \simeq N^3 / N_e^2$,[23] where N_e is the molecular weight between the entanglement points (if we set $N_e = N$ the results are identical to those for weak segregation). Because $1 \ll N/N_e$, the condition $H_Y \ll 1$ also holds in this case. However, one should note that the region of weak segregation becomes negligibly narrow for the case of reptation dynamics.

It is worth emphasizing that if one applies the present theory to other microphase structures such as lamellar, hexagonal and bcc structures, contributions to G'' linear in γ_0 do not appear. The amplitude equations corresponding to all these structures involve a single wavenumber because the magnitude of the fundamental reciprocal vectors of the lattices is determined by the condition $q^2 = 1$ (in dimensionless units). Because of this fact, the lowest contribution to the stress tensor in γ_0 vanishes as is readily seen from the formula (17). It is therefore interesting to see the feature that a linear stress–strain relation does exist and can be obtained for gyroid — as described in this paper — because of the existence of two fundamental modes with amplitudes A_j and B_j that have different magnitudes of the associated reciprocal lattice vectors. This is a necessary feature in the representation of the interconnected bicontinuous structure.

Although the present theory considers only the very idealized situations discussed above, it can be used as the starting point of a more elaborate analytical theory.

1) P. G. de Gennes and J. Prost: *The Physics of Liquid Crystals* (Clarendon Press, Oxford, U.K., 1993) 2nd ed.
2) M. W. Matsen and F. S. Bates: Macromolecules **29** (1996) 1091.
3) S. T. Hyde, S. Andersson, B. Ericsson, and K. Larsson: Z. Kristallogr. **168** (1984) 213.
4) R. Strey, R. Schomacker, D. Roux, F. Nallet, and U. Olsson: J. Chem. Soc., Faraday Trans. **86** (1990) 2253.
5) Y. Aota-Nakano, S. J. Li, and M. Yamazaki: Biochim. Biophys. Acta: Biomembranes **1461** (1999) 96.
6) A. M. Squires, R. H. Templer, J. M. Seddon, J. Woenkhaus, R. Winter, T. Narayanan, and S. Finet: Phys. Rev. E **72** (2005) 011502.
7) M. E. Vigild, K. Almdal, K. Mortensen, I. W. Hamley, J. P. A. Fairclough, and A. J. Ryan: Macromolecules **31** (1998) 5702.
8) C.-Y. Wang and T. P. Lodge: Macromolecules **35** (2002) 6997.
9) C. A. Tyler and D. C. Morse: Macromolecules **36** (2003) 8184.
10) K. Yamada and T. Ohta: Europhys. Lett. **73** (2006) 614.
11) T. Ohta, Y. Enomoto, J. L. Harden, and M. Doi: Macromolecules **26** (1993) 4928.
12) P. Chen and J. Viñals: Macromolecules **35** (2002) 4183.
13) F. Drolet, P. Chen, and J. Viñals: Macromolecules **32** (1999) 8603.
14) K. Yamada, M. Nonomura, and T. Ohta: Macromolecules **37** (2004) 5762.
15) T. Ohta and K. Kawasaki: Macromolecules **19** (1986) 2621.
16) K. Kawasaki and T. Ohta: Physica A **139** (1986) 223.
17) T. Ohta, H. Nozaki, and M. Doi: J. Chem. Phys. **93** (1990) 2664.
18) http://www.comp.tmu.ac.jp/k-yamada/double-gyroid/double-gyroid.html.
19) M. Doi and S. F. Edwards: *The Theory of Polymer Dynamics* (Oxford University Press, Oxford, U.K., 1986).
20) P. Pincus: J. Chem. Phys. **75** (1981) 1996.
21) K. Yamada, M. Nonomura, and T. Ohta: J. Phys.: Condens. Matter **18** (2006) L421.
22) Z.-F. Huang and J. Viñals: J. Rheol. **51** (2007) 99.
23) P. G. de Gennes: *Scaling Concepts in Polymer Physics* (Cornell University Press, Ithaca, NY, 1979).